BUERGER, M. J. (1951). In *Phase Transformations in Solids*. Edited by R. SMOLUCHOWSKI, J. E. MAYER & W. A. WEYL. New York: John Wiley.
BUERGER, M. J. (1961). *Fortschr. Mineral.* **39**, 9–23.
CHATTERJI, S., MACKAY, A. L. & JEFFERY, J. W. (1971). *J. Appl. Cryst.* **4**, 175.
CHRISTIAN, J. W. (1965). *The Theory of Transformations in Metals and Alloys*. Oxford: Pergamon.
EVDOKIMOVA, V. V. & VERESHCHAGIN, L. F. (1962). *Sov. Phys. JETP*, **43**, 1208–1212.
FRASER, W. L. & KENNEDY, S. W. (1972). *Acta Cryst.* B**28**, 3101.
HOVI, V. & VARTEVA, M. (1965). *Phys. Kondens. Mater.* **3**, 305–310.
KELLY, A. & GROVES, G. W. (1970). *Crystallography and Crystal Defects*. London: Longmans.
KENNEDY, S. W., PATTERSON, J. H., CHAPLIN, R. P. & MACKAY, A. L. (1974). *J. Solid State Chem.* **9** (No. 4). In the press.
LIEBERMAN, D. S. (1958). *Acta Met.* **6**, 680–693.
LIVSHITZ, L. D., RYABININ, Y. N., LARIONOV, L. V. & ZVEREV, A. S. (1969). *Sov. Phys. JETP*, **28**, 612–613.
LÜDEMANN, H. (1957). *Z. Naturforsch.* **12a**, 226–228.
MENARY, J. W., UBBELOHDE, A. R. & WOODWARD, I. (1951). *Proc. Roy. Soc.* A**208**, 158–169.
OWEN, W. S. & SCHOEN, F. J. (1971). *Structural Characteristics of Materials*, Chap. 4. Edited by H. M. FINNISTON. London: Elsevier.
PÖYHÖNEN, J. (1960). *Ann. Acad. Sci. Fenn.* A**VI**, No. 58.
PÖYHÖNEN, J., JAAKKOLA, S. & RÄSÄNEN, V. (1964). *Ann. Univ. Turku. A*, No. 80.
PÖYHÖNEN, J., MANSIKKA, K. & HEISKANEN, K. (1964). *Ann. Acad. Sci. Fenn.* A**VI**, No. 168.
PÖYHÖNEN, J. & RUUSKANEN, A. (1964). *Ann. Acad. Sci. Fenn.* A**VI**, No. 146.
RACHINGER, W. A. & COTTRELL, A. H. (1956). *Acta Met.* **4**, 109–113.
SHOJI, H. (1931). *Z. Kristallogr.* 77, 381–397.
WAYMAN, C. M. (1964). *Introduction to the Crystallography of Martensitic Transformations*. New York: Macmillan.
WECHSLER, M. S. (1959). *Acta Met.* **7**, 793–802.
WECHSLER, M. S., LIEBERMAN, D. S. & READ, T. A. (1953). *Trans. AIME*, **197**, 1503–1515.
ZINTL, E. & BRAUER, G. (1935). *Z. Electrochem.* **41**, 102–107.

Acta Cryst. (1974). A**30**, 22

Structural Studies by High-Resolution Electron Microscopy: Tetragonal Tungsten Bronze-Type Structures in the System Nb_2O_5–WO_3

BY S. IIJIMA*
Department of Physics, Arizona State University, Tempe, Arizona 85281, *U.S.A.*
AND J. G. ALLPRESS
Division of Tribophysics, CSIRO, University of Melbourne, Parkville, Victoria, 3052, *Australia*

(*Received* 14 *March* 1973; *accepted* 12 *April* 1973)

The contrast in many-beam lattice images from very thin crystals of $4Nb_2O_5.9WO_3$ is shown to be directly related to its known structure. On the basis of this correlation, the structure of $2Nb_2O_5.7WO_3$ is derived from the observed image contrast; it is an ordered intergrowth of the ReO_3 and tetragonal tungsten bronze structural types. The structures of typical fault boundaries and disordered intergrowths are described, and those of the reported compounds $6Nb_2O_5.11WO_3$ and $3Nb_2O_5.8WO_3$ are discussed.

1. Introduction

The binary system Nb_2O_5–WO_3 has been the subject of a great deal of structural investigation during recent years, and at least ten distinct phases have been recognized by X-ray methods (Roth & Waring, 1966). The dominant structural unit in all these phases is the MO_6 octahedron, which, in general, shares its corner oxygen atoms with neighbours to build up a three-dimensional lattice. In one crystallographic direction through the structures, the octahedra always form linear strings, with a simple repeat distance of about 0·38 nm, corresponding to the length of a body diagonal. Differences between the structures arise from variations in the arrangement of octahedra in the remaining two directions, and two major structural types can be distinguished:

(*a*) Crystallographic shear (CS) structures, in which the octahedra are joined as in ReO_3 [Fig. 1(*a*)], into blocks or slabs, and neighbouring slabs are joined by sharing octahedral edges rather than corners. This description applies to the Magnéli phases (>90 mole % WO_3), and to the Nb_2O_5-type of block structures (<48 mole % WO_3).

(*b*) Tunnel structures, in which the octahedra are joined in a more complex way, leaving tunnels of various shapes, some of which may be filled by additional ions. These include WNb_2O_8, and several structures containing 64–78 mole % WO_3, which share a common

* On leave from the Research Institute for Scientific Measurements, Tohoku University, Sendai, Japan.

tetragonal tungsten bronze (TTB) type of host lattice [Fig. 1(*b*)].

In both the CS and tunnel structures, the basic lattice of corner-shared octahedra has the stoichiometry MO_3. The reduction in overall O/M ratio required by the composition $x Nb_2O_5 . y WO_3$ is achieved by edge-sharing of octahedra in the CS structures, and by filling of some of the pentagonal tunnels with strings of composition MO in the tunnel structures.

During an investigation of these phases by electron microscopy at moderate resolution (*ca.* 0·7 nm), it was found (Allpress, Sanders & Wadsley, 1969) that lattice images of the CS structures contained contrast which could be correlated directly with structural features. In particular, the CS planes were readily distinguished, because of their higher-than-average charge density. The application of similar methods to the TTB structures (Allpress, 1969*a*, 1972), while not leading to the same degree of successful correlation between image and structure, has nevertheless revealed the presence of twin and out-of-phase boundaries in these materials, and provided evidence for disorder, and for intergrowth between the TTB and ReO_3-type structures.

More recently, studies of CS structures at improved resolution (*ca.* 0·3 nm, Iijima 1971, 1973; Iijima & Allpress, 1973) have indicated the possibility of resolving the small square tunnels *within* the ReO_3-type blocks [Fig. 1(*a*)]. We have therefore turned our attention to the TTB-type structures, in the hope that we could distinguish between filled and empty pentagonal tunnels, and throw further light on some of the ordered and defect structures which we have studied previously at lower resolution.

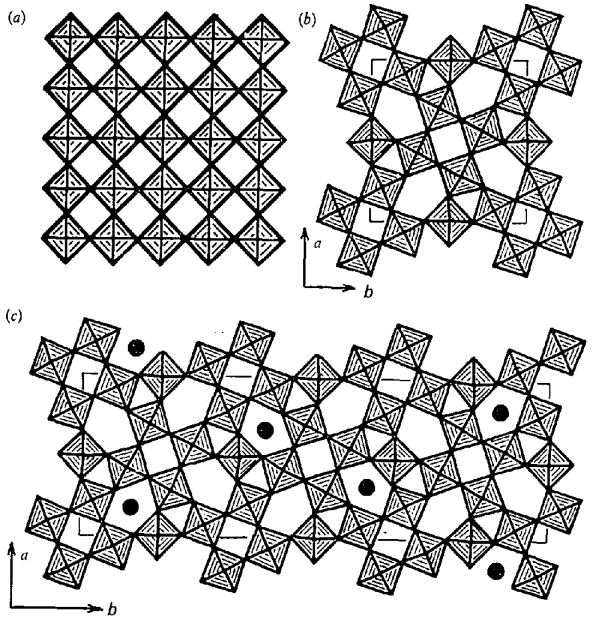

Fig. 1. Structural elements encountered in the binary system $Nb_2O_5 . WO_3$. Each hatched square represents a MO_6 octahedron, which shares its corner oxygen atoms with neighbouring octahedra to form a lattice of composition MO_3. The cubic ReO_3 structure is shown in (*a*), and the host lattice of tetragonal tungsten bronze (TTB) in (*b*). The structure of $4Nb_2O_5 . 9WO_3$, shown in (*c*), contains three TTB subcells, and the superlattice is a consequence of the ordered occupation of one third of the pentagonal tunnels by –O–M–O–M–O strings parallel to c (filled circles).

Crystallographic data for the four known mixed oxides of niobium and tungsten which are reported to possess TTB-type structures are given in Table 1, together with that for tetragonal potassium tungsten bronze. Of these four structures, that of the 4:9 compound (*i.e.* $4Nb_2O_5 . 9WO_3$) has been most extensively studied, and will be used for our interpretations. Its structure (Sleight, 1966) is shown in Fig. 1(*c*). It contains three TTB-type subcells, and a superlattice which is a consequence of the ordered filling of one third of the pentagonal tunnels. An alternative tetragonal structure containing nine subcells has also been suggested (Craig & Stephenson, 1969), but our previous studies have indicated clearly that the true unit cell is the orthorhombic cell given in Table 1, and that the nine-subcell unit is probably an artifact due to extensive microtwinning.

In this paper, we will confine ourselves to four aspects of the results:

(*a*) The experimental correlation of the lattice image contrast with structure for the 4:9 compound.

(*b*) The use of this correlation to derive the structure of the 2:7 compound, for which the structure shown in Fig. 6(*a*) had been proposed (Stephenson, 1968) without proof.

(*c*) The structure and composition of crystals containing fault boundaries, and exhibiting intergrowth of the above structures.

(*d*) Observations on a sample whose composition lay close to that of the 6:11 compound in Table 1.

Table 1. *Crystallographic data for* K_xWO_3 *and related* Nb, W *oxides*

Compound	Symmetry*	Space group	Unit-cell dimensions (nm)			Reference
			a	*b*	*c*	
$K_xWO_3 (x = 0{\cdot}5)$	*T*		1·230		0·384	Magnéli (1949)
$4Nb_2O_5 . 9WO_3$	*O*	$P2_12_12$	1·2251	3·6621	0·394	Sleight (1966)
$6Nb_2O_5 . 11WO_3$	*O*	$P2_12_12$	1·220	3·674	0·3951	Stephenson (1968)
$2Nb_2O_5 . 7WO_3$	*T*		2·426		0·3924	Roth & Waring (1966)
$3Nb_2O_5 . 8WO_3$	*T*		1·219		0·3968	Waring (1966)

* *T*, Tetragonal.
O, Orthorhombic.

2. Experimental

The samples were provided by the late Dr A. D. Wadsley, and were part of a series of preparations used to identify the phases present in the Nb_2O_5–WO_3 system (Roth & Wadsley, 1965). They were obtained by heating appropriate mixtures of the two component oxides in sealed platinum capsules at temperatures of 1400–1700°K for periods of at least 18 h and quenching the products. Their nominal compositions were $Nb_2O_5:WO_3 = 13:24$, 3:7, 17:48 and 19:63.

Thin fragments from these samples were prepared by grinding, dispersed on perforated carbon films supported on specimen grids, and examined in a JEM 100B electron microscope, as described previously (Iijima, 1973). Micrographs were recorded from very thin regions of fragments whose orientations were adjusted so that the electron beam was incident exactly parallel to the short (0·38 nm) axis. Focusing conditions were about 90 nm underfocus from the Gaussian image plane, and up to 120 diffracted beams were included by the objective aperture and allowed to contribute to the images.

3. Results and interpretation

3.1. $4Nb_2O_5.9WO_3$

A high-resolution lattice image from the 4:9 phase is reproduced in Fig. 2(*a*). It consists of an array of white patches set in a darker background, and the repeating unit of contrast is outlined by a rectangle. The size of this rectangle corresponds to that of the unit cell, as determined from X-ray data (Table 1).

Our experience with CS structures has shown that for the conditions under which the micrographs are recorded, the contrast in high-resolution underfocus images can be interpreted directly in terms of structure, and that empty tunnels in the ReO_3-type blocks appear as white dots in the images. A satisfactory interpretation of the contrast in Fig. 2(*a*) is obtained if a similar correlation between white patches and empty tunnels in the structure is assumed. In Fig. 2(*b*), the structural drawing in Fig. 1(*c*) is shown superimposed on the repeating unit of the lattice image. The correspondence between white patches and empty square and pentagonal tunnels is quite good, as is that of dark areas and filled pentagonal tunnels (circles) and octahedra.

3.2. *Fault boundaries in* $4Nb_2O_5.9WO_3$

The presence of domain boundaries of several types in this material was established by earlier observations at lower resolution (Allpress, 1969*a*, 1972). The present results show sufficient detail to enable us to derive convincing models for the structure of these boundaries, and to determine their influence on the overall stoichiometry of the crystals. An example of an image from a faulted crystal is shown in Fig. 3. Where possible, the image is divided into rectangular areas corresponding to unit cells of the 4:9 phase. However, along the ⟨110⟩ directions marked by arrows, there are eight regions (circled) in which the contrast differs slightly from that of the matrix. Within each of these regions, there are four white patches surrounding a smaller central patch, and our correlation with empty tunnels suggests that these areas correspond to subcells of the TTB-type host lattice in which *all* the tunnels are empty. These subcells differ from those in the ordered structure, because in the latter, one or two of the four pentagonal tunnels in each subcell are occupied.

A model of this fault boundary is shown in Fig. 3(*b*). It is obvious that the TTB-type host lattice is continuous across the boundary, and that the fault is due to a displacement of one third of a unit cell along **b** (or one tetragonal subcell) in the arrangement of filled pentagonal tunnels. This displacement may be regarded as an out-of-phase boundary lying along [110] and [$\bar{1}$10].

Since we are able to distinguish between occupied and empty tunnels, the influence of the out-of-phase boundary on the composition of the crystal can be determined. If we assume that the host lattice is perfect and that occupied tunnels are completely filled, the overall composition can be written $x(M_{10}O_{30})_h.y(MO)_t$, where the subscripts h and t refer to the host lattice and tunnel components respectively. In the ordered 4:9 structure [Fig. 1(*c*)], $x=3$ and $y=4$. In both the [110] and [$\bar{1}$10] boundaries in Fig. 3, repeating units containing 5 TTB subcells and 6 filled tunnels can be distinguished; *i.e.* $x=5$, $y=6$. The corresponding $Nb_2O_5:WO_3$ ratio is 3:8 or 0·367, which is considerably lower than that for the ordered compound (0·445). We may therefore conclude that this particular crystal contains a slight excess of WO_3. This result is consistent with the fact that the crystal was found in a multiphase mixture of nominal composition $19Nb_2O_5.63WO_3$ (*i.e.* ratio = 0·302).

In addition to out-of-phase boundaries, several different types of twin boundaries were observed, and their structures and compositions can be analysed in a similar way. For example, Fig. 4(*a*) shows a boundary separating domains in which the unit cells (marked *A* and *B*) are related by a rotation of 90° about [001]. Again, the TTB-type host lattice is continuous, and the model in the inset shows only the pattern of filled and empty pentagonal tunnels, which are represented by full and open circles respectively. The boundary region is a parallel-sided slab of structure lying along $[010]_A$ (or $[100]_B$), and within its repeating unit (dashed outline), $x=6$ and $y=7$. The calculated $Nb_2O_5:WO_3$ ratio is 14:39 or 0·359. In Fig. 4(*b*), the unit cells *A* and *B'* are related by a mirror plane along $(\bar{3}10)_A$ [or $(\bar{3}10)_{B'}$]. Within the boundary region, the two unit cells overlap, and share a filled tunnel. The composition of the boundary region varies, because the tunnels marked by arrows appear to be sometimes filled and sometimes empty. The dashed line in the inset marks an area of boundary which contains the equivalent of 9 TTB subcells and 11 filled tunnels, having the overall composition ratio $Nb_2O_5:WO_3 = 22:57 = 0·386$. Similar areas further along the boundary contain 12 filled tunnels,

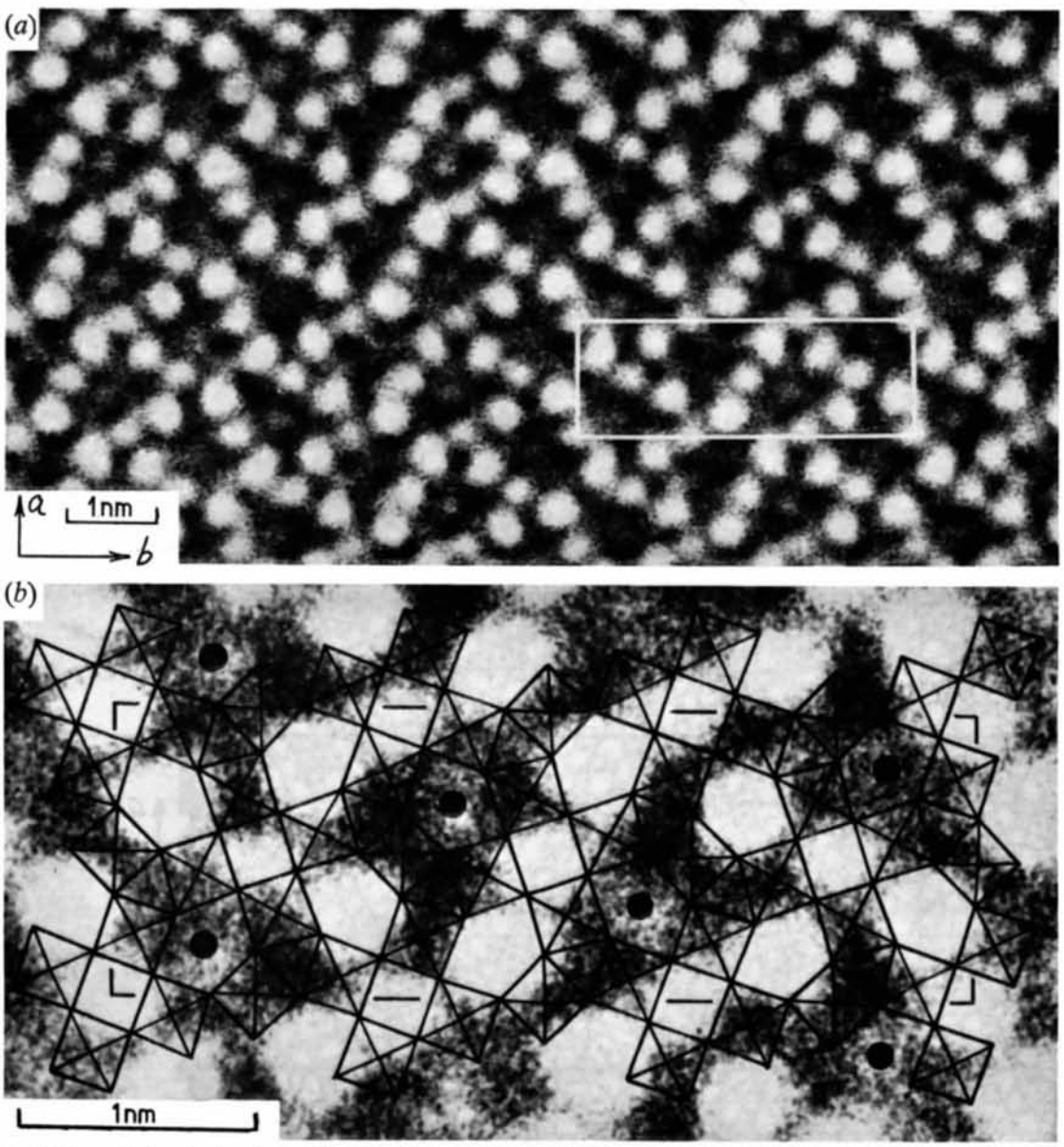

Fig. 2. (*a*) High-resolution lattice image from a thin crystal of $4Nb_2O_5.9WO_3$. The repeating unit of contrast is outlined. (*b*) The structure of $4Nb_2O_5$ $9WO_3$ [Fig. 1(*c*)] superimposed on an enlarged portion of (*a*). Note the correspondence between white patches in the image and empty square and pentagonal tunnels in the structure.

[*To face p.* 24

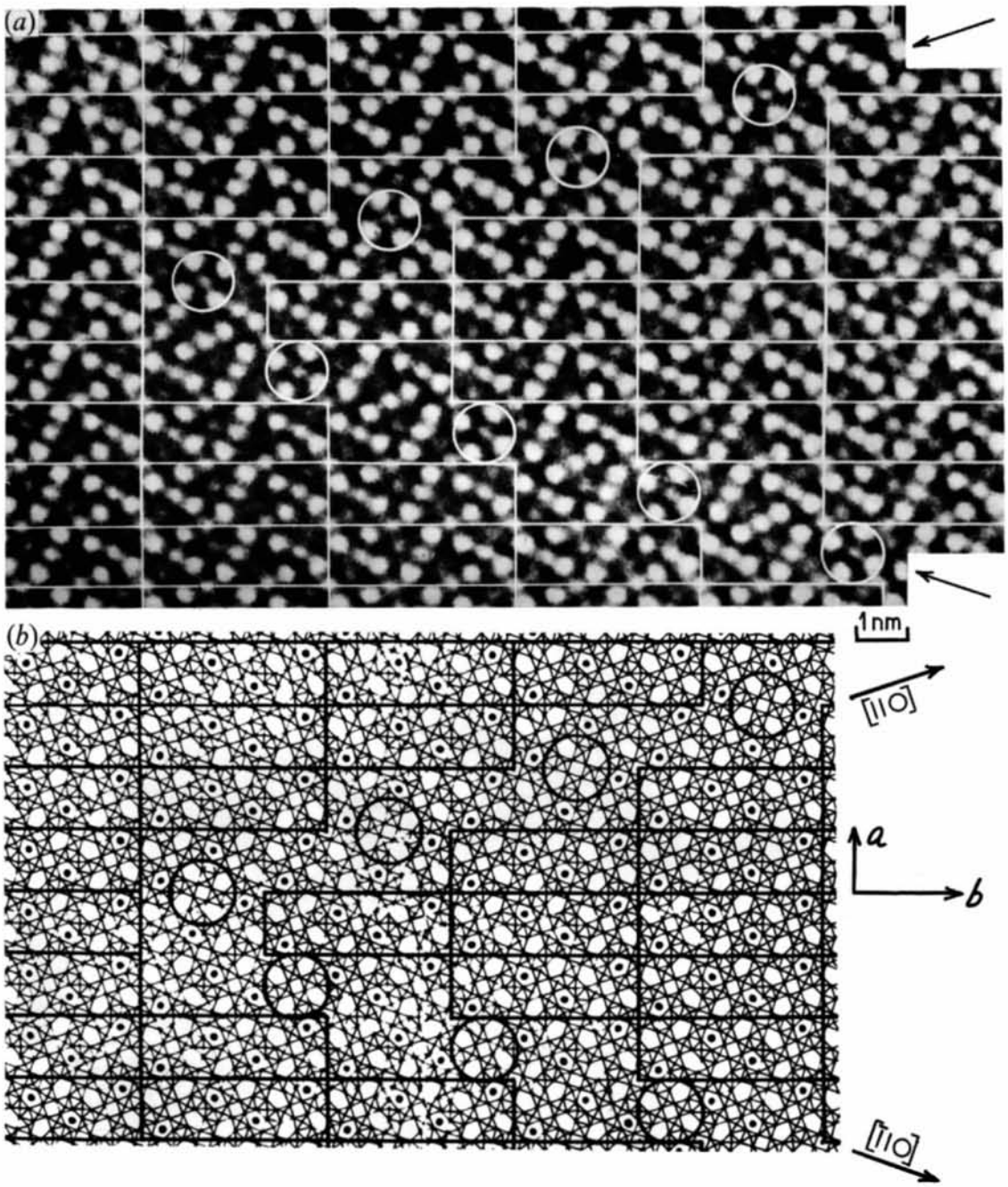

Fig. 3. Lattice image from a crystal of $4Nb_2O_5.9WO_3$ containing a zigzag out-of-phase boundary (arrowed). Rectangles outline unit cells of the ordered structure, and circles within the boundary mark TTB subcells in which all four pentagonal tunnels are empty. The presence of the boundary causes a displacement of $\frac{1}{4}[010]$ in the ordered structure. (*b*) Model of the boundary structure, derived from the contrast in (*a*). The host lattice of corner-shared octahedra is continuous, but the pattern of occupied tunnels (full circles) is interrupted at the boundary.

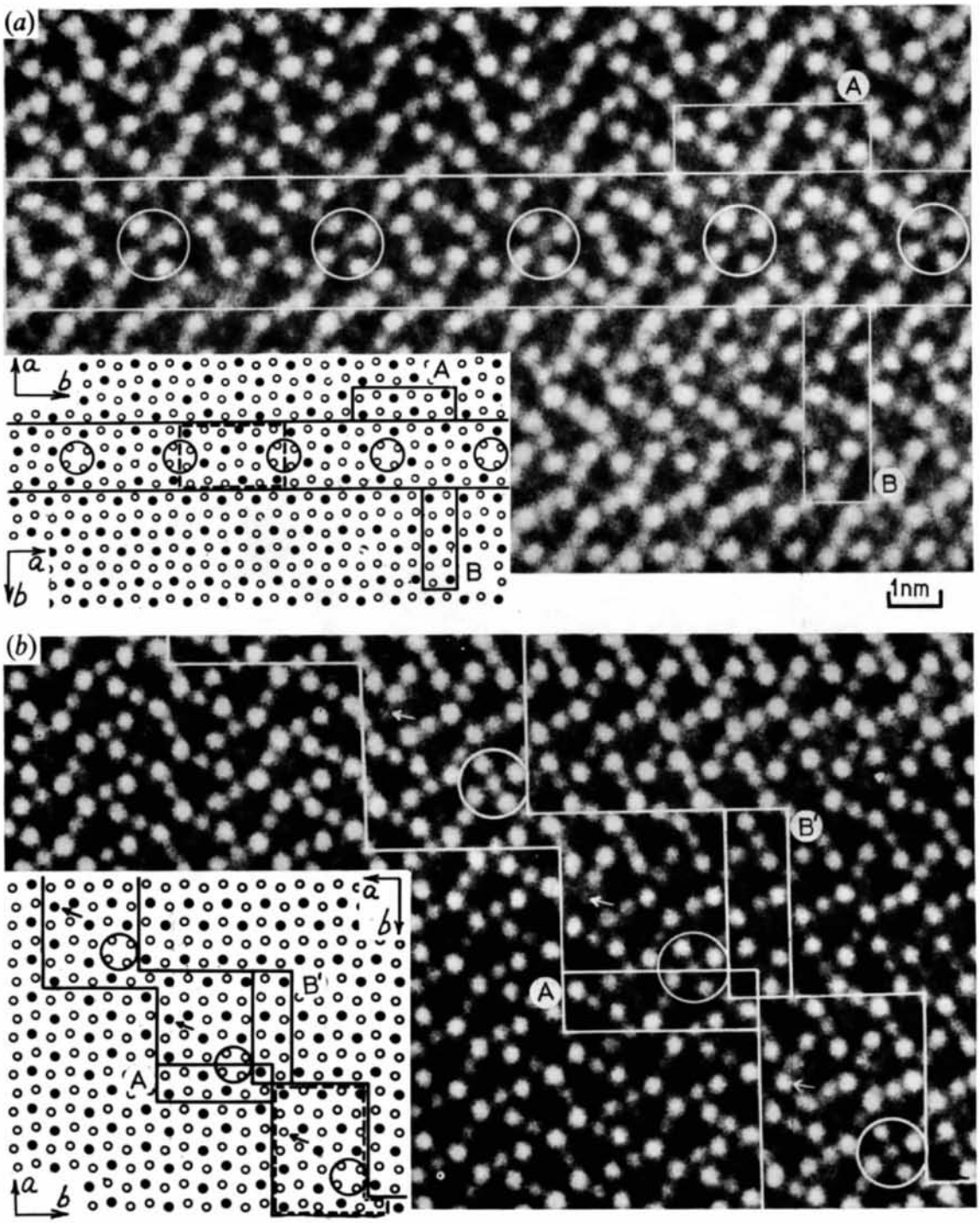

Fig. 4. Twin boundaries in $4Nb_2O_5.9WO_3$. The boundary regions which contain empty TTB subcells (circled) are outlined, and unit cells of the ordered structure on either side of the boundaries are also marked A, B and B'. The insets show the arrangement of occupied and empty pentagonal tunnels as full and open circles respectively. In (a), the domains A and B are related by a rotation of 90° about [001], and in (b), A and C' are related by a mirror plane on $(\bar{3}10)$. Tunnels marked by arrows in (b) are sometimes occupied and sometimes empty.

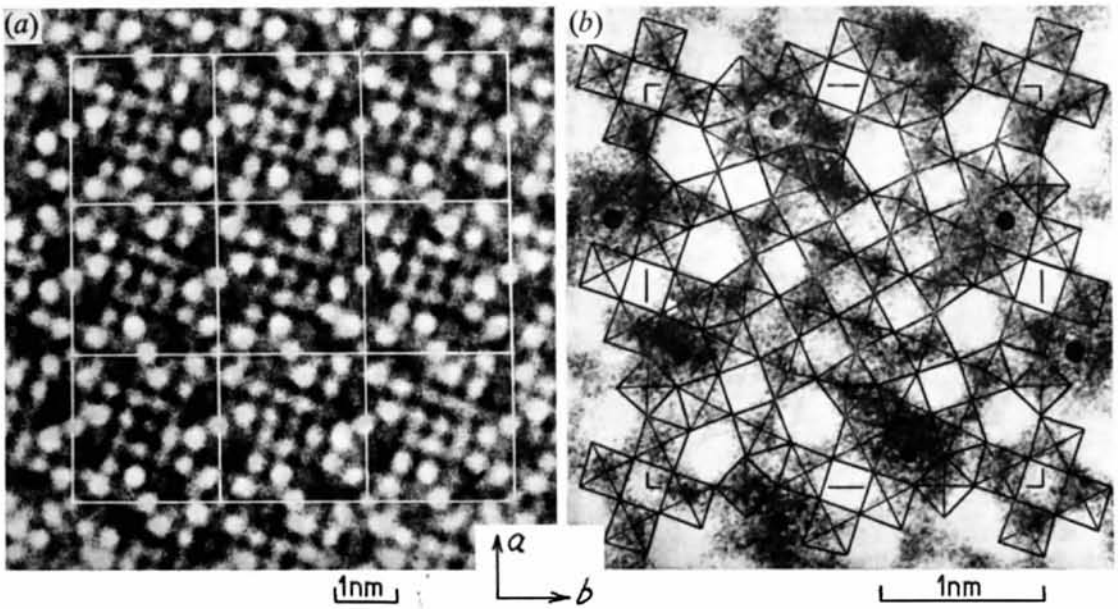

Fig. 5. (*a*) High resolution lattice image from a thin crystal of $2Nb_2O_5.7WO_3$. The squares outline repeating units of contrast. (*b*) The proposed structure of $2Nb_2O_5.7WO_3$ [see Fig. 6(*b*)], superimposed on an enlargement of part of (*a*) showing satisfactory correspondence between empty tunnels in the structure and white patches in the image.

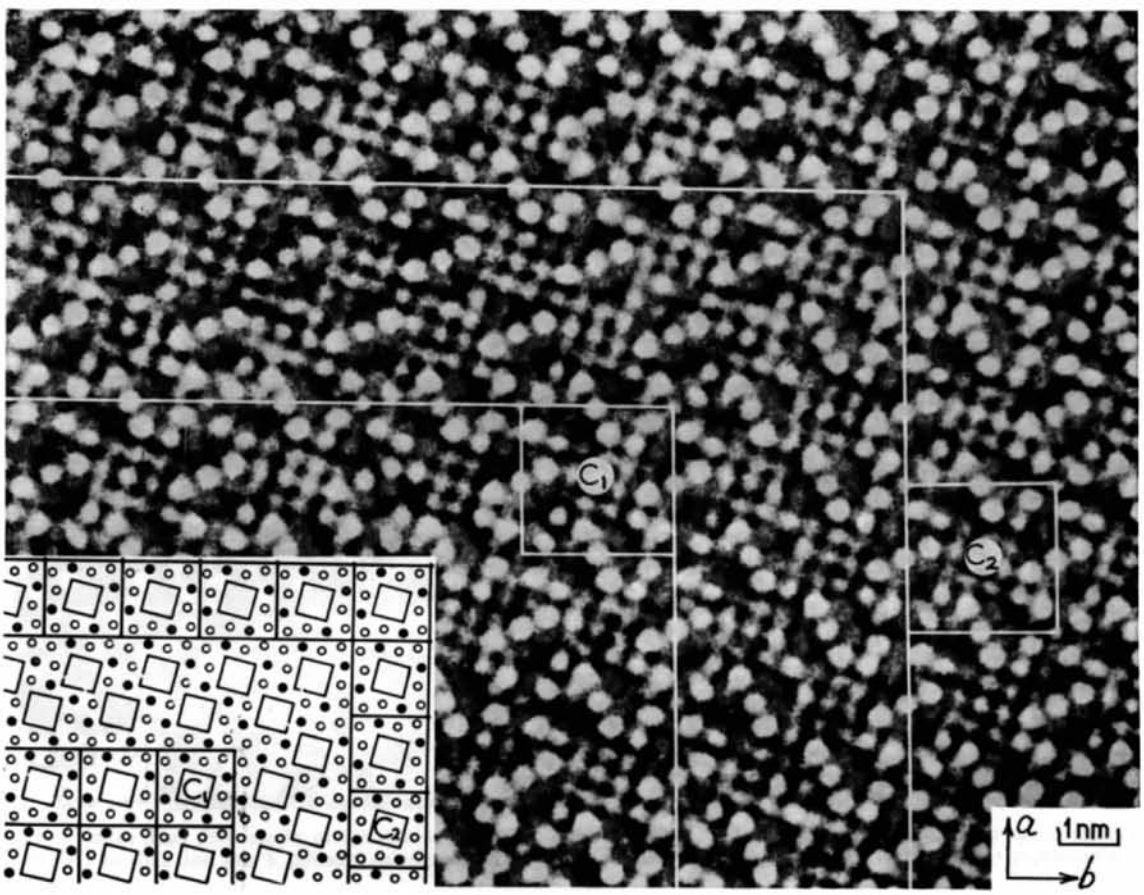

Fig. 7. Antiphase boundary in $2Nb_2O_5.7WO_3$. The domains C_1 and C_2 are displaced by $\frac{1}{2}[110]$ with respect to each other, and the boundary has the same composition as the matrix.

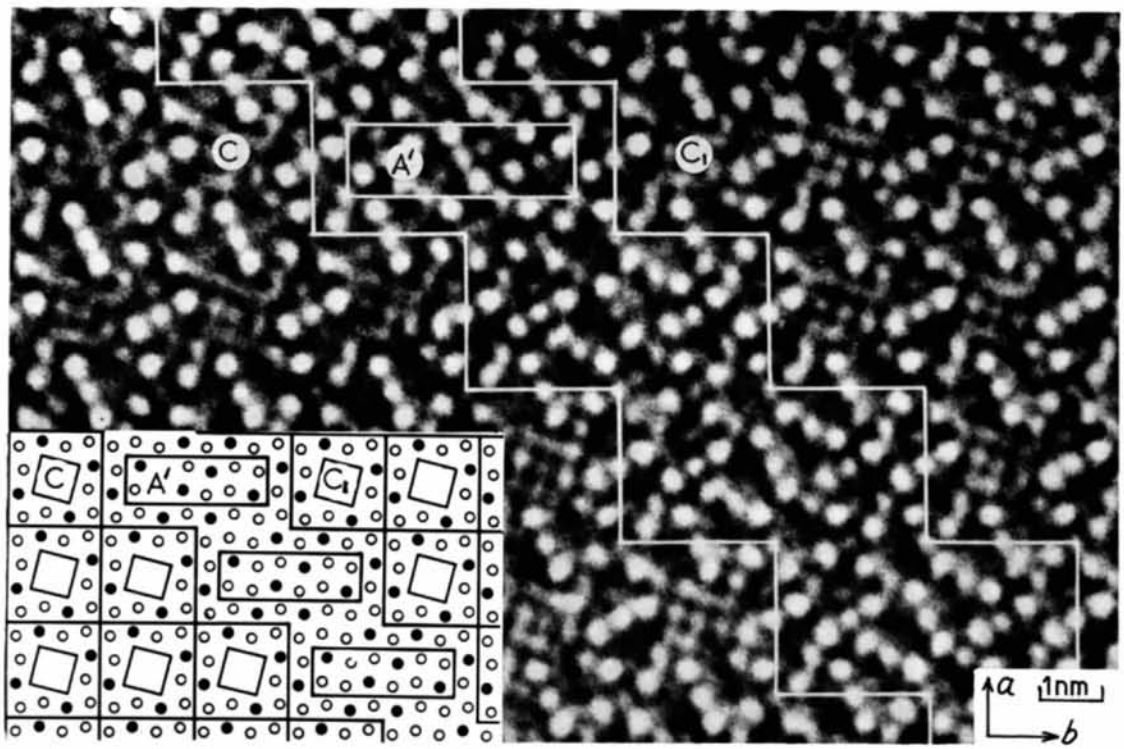

Fig. 8. Lattice image showing domains of $2Nb_2O_5.7WO_3$, labelled C and C_1, which are in phase with each other, but are separated by a boundary (outlined) whose composition is $2Nb_2O_5.5WO_3$. The rectangles labelled A' are unit cells of $4Nb_2O_5.9WO_3$.

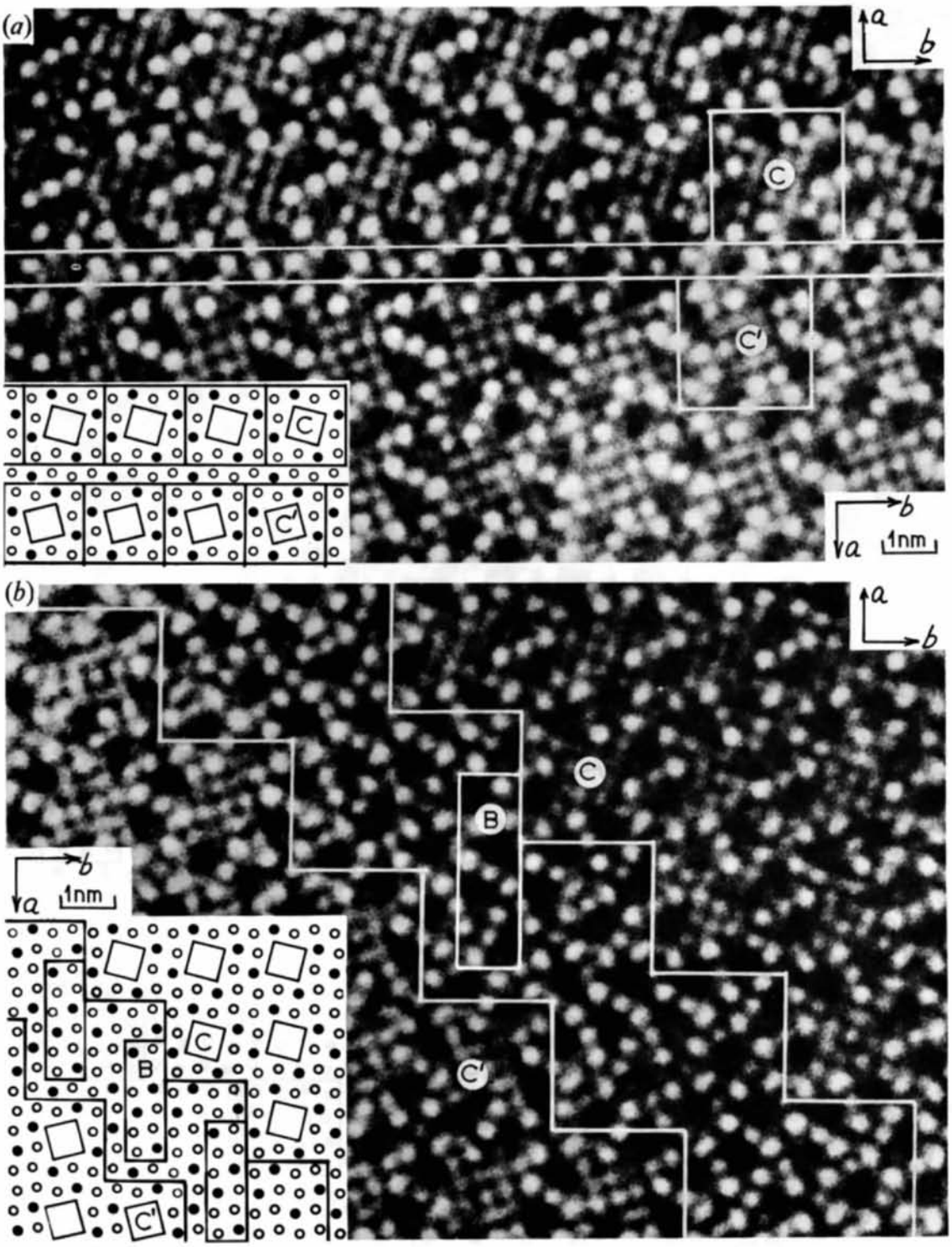

Fig. 9. Out-of-phase domainsin 2 Nb_2O_5.7WO_3. Unit cells in the regions *C* and *C'* are related by a mirror plane on (010). In (*a*), the domain boundary (outlined) lies along [010] and has the same composition as the matrix. In (*b*), the boundary is stepped along [110] and its composition is $2Nb_2O_5.5WO_3$. It contains unit cells (*B*) of $4Nb_2O_5.9WO_3$, and is very similar to the boundary in Fig. 8.

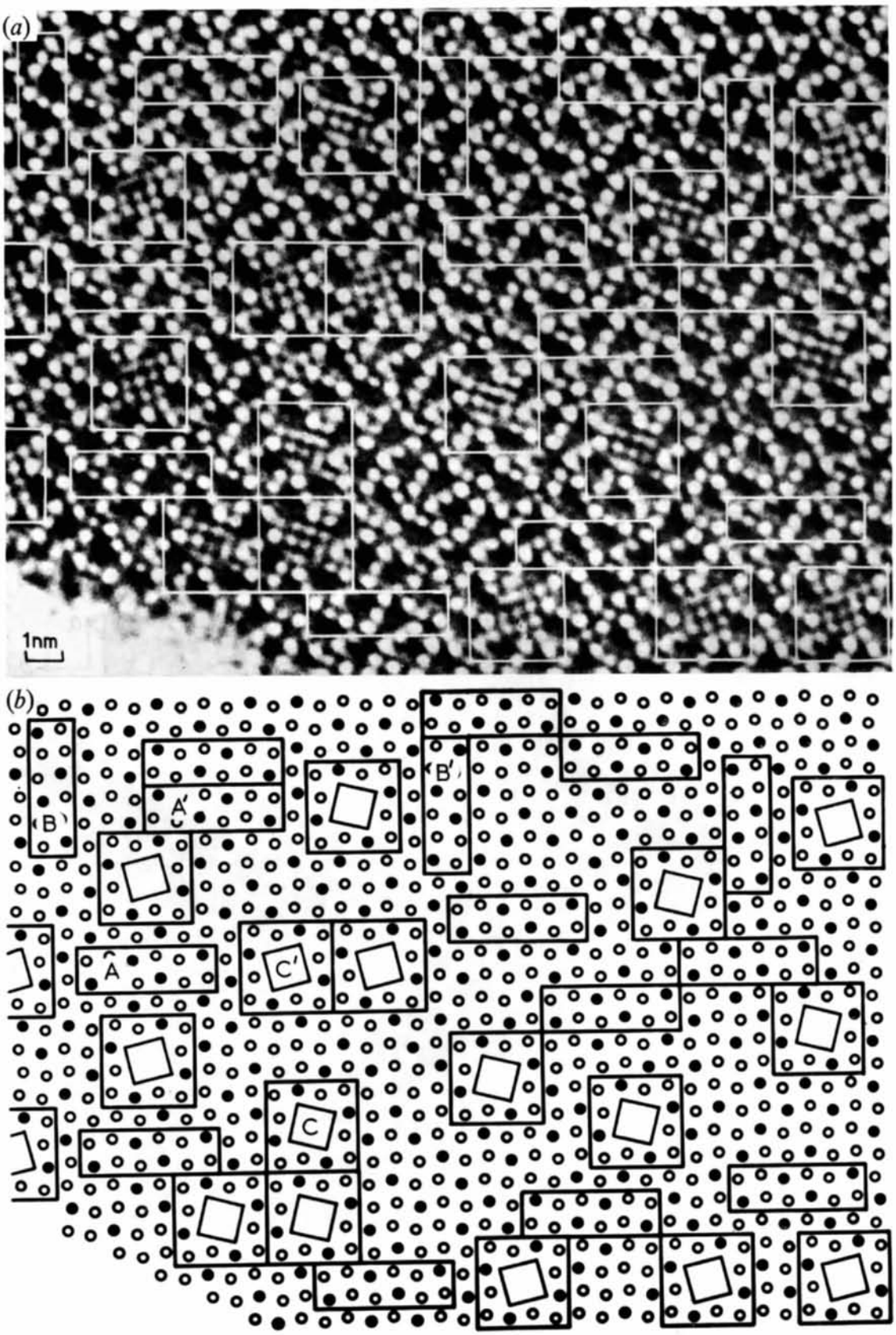

Fig. 10. (*a*) Lattice image from a thin fragment of nominal composition $17Nb_2O_5.48WO_3$, showing disordered occupancy of pentagonal tunnels over the whole region, but a strong tendency for short-range order over more limited areas. Unit cells of both $4Nb_2O_5.9WO_3$ and $2Nb_2O_5.7WO_3$ are outlined. (*b*) Model of the structure derived from (*a*), showing occupied and empty pentagonal tunnels as full and open circles respectively, and 4×4 blocks of ReO_3-type structure as small squares. Unit cells of the two ordered phases are outlined, and labelled *A*, *A'*, *B*, *B'*, *C*, *C'*, according to their orientations, in the same way as in Fig. 4 and 9.

giving a ratio 24:54=4:9, the same as that of the matrix. This boundary is therefore only very slightly non-stoichiometric with respect to the matrix. Both images in Fig. 4 were recorded from fragments of nominal composition $3Nb_2O_5.7WO_3$ (ratio=0·43), slightly richer in WO_3 than the 4:9 phase; it therefore seems that the fault boundaries can act as sinks for this discrepancy in composition.

3.3. $2Nb_2O_5.7WO_3$

A high-resolution lattice image from a thin fragment of this phase is reproduced in Fig. 5(*a*), and the square repeating unit, about 2·4 nm on a side, is outlined. Its size corresponds to that of the tetragonal unit cell of the phase $2Nb_2O_5.7WO_3$. Fragments with this structure were the major component in the mixture of composition $19Nb_2O_5.63WO_3$.

At the corners of the repeating unit in Fig. 5(*a*), there are groups of four white patches surrounding a smaller central patch, very similar indeed to those encircled in Figs. 3(*a*), 4, which we identified as TTB-type subcells with all tunnels empty. Centred on the midpoints of the edges of the repeating unit are linear groups of three white patches, similar to those which lie across the corners and centre of unit cells in lattice images from $4Nb_2O_5.9WO_3$ [Figs. 2(*a*), 3(*a*)]. By analogy, they probably correspond to TTB-type subcells with two opposite pentagonal tunnels occupied. In the centre of the square in Fig. 5(*a*), there is a square array of nine white patches, and the separation between the four central dark blobs is about 0·38 nm. This contrast resembles that expected from a 4×4 block of corner-shared octahedra of the ReO_3-type structure (Iijima & Allpress, 1973*a*).

On the basis of a limited amount of X-ray evidence, and prior knowledge of related structures, Stephenson (1968) predicted that $2Nb_2O_5.7WO_3$ should have the structure shown in Fig. 6(*a*). The unit cell contains four TTB-type subcells, and one quarter of the pentagonal tunnels are filled. In most respects, this structure is consistent with our interpretation of the lattice image contrast. The subcells which are centred on the corners of the unit cell (*e.g.* the dashed square) all contain empty tunnels, and those centred half way along the cell edges contain two filled tunnels, in the correct orientation to match the lattice image contrast.

However, the central part of the proposed structure is obviously incorrect; some rearrangement of the octahedra is required in order to produce a 4×4 block of ReO_3-type material in this region. This requirement is achieved very simply, by rotating the central four octahedra [circled in Fig. 6(*a*)] clockwise by about 45°, and making slight adjustment to the orientations of the surrounding octahedra. By this means, all the triangular and pentagonal tunnels around the circumference of the circle in Fig. 6(*a*) are converted to approximately square tunnels [Fig. 6(*b*)], and the 4×4 block of ReO_3-type material is produced. In Fig. 5(*b*), this revised structure is superimposed on the lattice image, and the correspondence between empty tunnels and white patches is clearly very good.

The symmetry of the revised structure shown in Fig. 6(*b*) is tetragonal, space group $P4$, and all atoms lie in the general positions 4(*d*), with $z=0$ for metal and $z=\frac{1}{2}$ for oxygen. The x and y coordinates of the atoms in TTB-type positions were derived from those quoted for barium strontium niobate (TTB-type, Jamieson, Abrahams & Bernstein, 1968), while those of atoms in

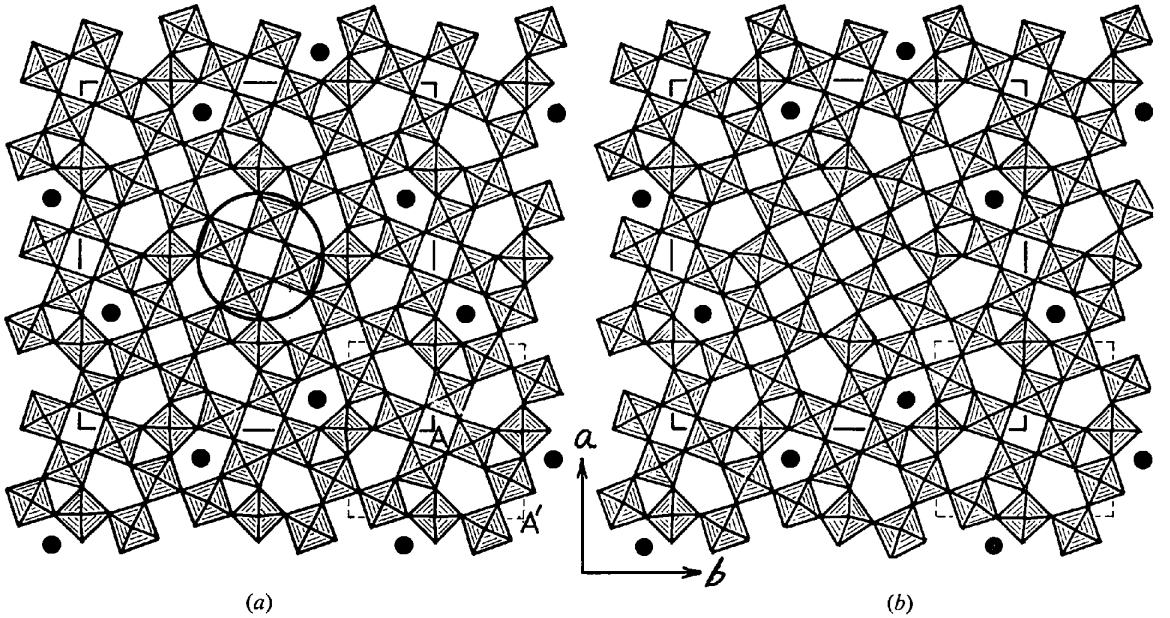

(*a*) (*b*)

Fig. 6. Proposed structures for $2Nb_2O_5.7WO_3$. (*a*) According to Stephenson (1968). (*b*) Stephenson's structure, modified by rotating the central group of four octahedra circled in (*a*) as indicated by the observed lattice image contrast (Fig. 5).

the central ReO_3-type region were chosen to give reasonable geometry. These coordinates are given in Table 2, but they must be regarded as very approximate, and suitable only as a starting point for any future refinement of X-ray data.

3.4. *Fault boundaries in* $2Nb_2O_5.7WO_3$

The concentration of fault boundaries in $2Nb_2O_5.7WO_3$ was much higher than in $4Nb_2O_5.9WO_3$, as was the number of different observed structures. Several typical examples are shown in Figs. 7–9. In all cases, the host lattice of TTB-type structure is basically continuous, and therefore the structural models in these and subsequent figures show only the positions and occupancies of pentagonal tunnels (open circles = empty, filled circles = occupied) and the positions of 4×4 blocks of ReO_3-type material (squares). Unit cells are outlined by heavy lines.

The lattice image in Fig. 7 shows two domains of $2Nb_2O_5.7WO_3$, labelled C_1 and C_2, which are displaced by half a unit cell with respect to each other along both [100] and [010]. The boundary is therefore one type of antiphase domain boundary, and its structure is shown in the inset. It is easy to demonstrate that, in spite of the fact that the ReO_3-type blocks are closer together in the boundary than they are in the matrix, the composition of the boundary region is the same as that of the matrix.

The lattice image in Fig. 8 shows domains C and C_1, which remain in phase with each other, although separated by a stepped boundary along $[\bar{1}10]$, which does not contain any ReO_3-type blocks. The structure of this boundary is shown in the inset and its composition is $2Nb_2O_5.5WO_3$, which is considerably richer in Nb_2O_5 than the matrix. Within the boundary structure, rectangular unit cells of $4Nb_2O_5.9WO_3$ (*e.g.* A') can be distinguished.

Examples of a third type of boundary are shown in Fig. 9. The domains C and C' on either side of these boundaries are related by a mirror plane on (100), and are also displaced by a quarter of a unit cell along [100] and [010] with respect to each other. In Fig. 9(*a*), the boundary is very narrow and parallel to (100), and has the same composition as the matrix. In Fig. 9(*b*), it is stepped along [110] and has the composition $2Nb_2O_5.5WO_3$. The boundary in Fig. 8 has the same composition and direction, and a similar structure.

3.5. *Disordered intergrowths of* $4Nb_2O_5.9WO_3$ *and* $2Nb_2O_5.7WO_3$

In many cases, the domain structures described so far were not fully developed, and we observed small groups or isolated unit cells of one or both of the ordered structures distributed randomly in a continuous TTB-type host matrix. This was particularly true of the sample of nominal composition $17Nb_2O_5.48WO_3$, intermediate between those of the two ordered phases.

A lattice image from a disordered fragment is reproduced in Fig. 10(*a*). A careful examination of the contrast indicated that again, the TTB-type host lattice is continuous, and that variations in contrast could be attributed to the non-periodic arrangement of filled pentagonal tunnels and 4×4 blocks of ReO_3-type structure. A model in which these features are marked is shown in Fig. 10(*b*), and it is a simple matter to identify unit cells (outlined) of $4Nb_2O_5.9WO_3$ (rectangular) and $2Nb_2O_5.7WO_3$ (square). These unit cells are of two types, those marked with a superscript being the mirror images of the others. It will be noted that all cells of the same type are displaced from one another by integral subcell vectors, while dissimilar cells are displaced by half integral subcell vectors. These relationships arise because the TTB subcell has two possible origins [marked A and A' in Fig. 6(*a*)] which lie $\frac{1}{2}\langle110\rangle_s$ apart, and both the subcells and the superstructures derived using these origins are mirror-related to one another. In the case of $4Nb_2O_5.9WO_3$, there is the additional possibility that the cell can be rotated by 90° about [001], and this occurs at B in Fig. 10(*b*).

The composition of a region such as is shown in

Table 2. *Approximate coordinates of atoms in the structure of* $2Nb_2O_5.7WO_3$

Space group $P4$, all atoms in 4(*d*); x, y, z; $\bar{x}, \bar{y}, z$; $y, \bar{x}, z$; $\bar{y}, x, z$.

	x	y		x	y		x	y
M(1)	0·086	0·336	O(12)	0·078	0·253	O(22)	0·284	0·319
M(2)	0·037	0·106	O(13)	0·498	0·173	O(23)	0·216	0·182
M(3)	0·144	0·213	O(14)	0·003	0·328	O(24)	0·140	0·390
M(4)	0·287	0·144	O(15)	0·253	0·423	O(25)	0·360	0·110
M(5)	0·394	0·037	O(16)	0·248	0·078	O(26)	0·110	0·140
M(6)	0·106	0·463	O(17)	0·069	0·034	O(27)	0·400	0·448
M(7)	0·213	0·356	O)18)	0·319	0·216	O(28)	0·338	0·473
M(8)	0·356	0·287	O(19)	0·182	0·284	O(29)	0·428	0·270
M(9)	0·25	0	O(20)	0·466	0·069	O(30)	0·480	0·425
M(10)	0·5	0·25	O(21)	0·034	0·432	O(31)	0·380	0·375
M(11)	0·173	0·003						

O(1–11), same parameters as M(1–11), but with $z=0$.
M(1–11), O(12–31), $z=\frac{1}{2}$.

Fig. 10 can be readily estimated by counting the numbers of subcells and filled tunnels. The model in Fig. 10(*b*) contains 258 subcells, and 301 filled tunnels, and the corresponding composition is $602Nb_2O_5.1677WO_3$. The $Nb_2O_5:WO_3$ ratio is therefore 0·359, which is in reasonable agreement with the nominal value (0·354) for the sample of $17Nb_2O_5.48WO_3$.

In addition to the disordered intergrowth which we have just described, many fragments in the WO_3-rich specimens contained extended domains of ReO_3-type material, coherently intergrown with regions of TTB-type structure, and sharing a common 0·38 nm axis. These domain structures have already been described briefly (Allpress, 1972) and will be discussed in detail in a subsequent paper (Iijima & Allpress, 1974).

3.6. '$6Nb_2O_5.11WO_3$'

A further TTB-type phase whose composition lies close to $6Nb_2O_5.11WO_3$ has been reported (Roth & Wadsley, 1965; Roth & Waring, 1966). Apart from a difference in colour, this phase appears to be almost indistinguishable from $4Nb_2O_5.9WO_3$. As Table 1 indicates, their space groups and unit-cell dimensions correspond closely, and the positions and intensities of the lines in their X-ray powder patterns (Roth & Waring, 1966) are also very similar. More recently, Stephenson (1968) examined a 'single' crystal of $6Nb_2O_5.11WO_3$ by X-ray methods, and concluded that it was in fact an intergrowth of two stable phases; orthorhombic $9Nb_2O_5.16WO_3$ and monoclinic $9Nb_2O_5.17WO_3$. Although he was unable to prepare separate identifiable phases at either of these compositions, he proposed that in the 6:11 compound, small domains of ordered intergrowth, consisting of slabs of the 9:16 and 9:17 structures stacked regularly along the *c* axis, could give rise to a 'domain unit cell' with the dimensions $a=1·2195$, $b=3·674$, $c=3·1608$ nm (*cf.* Table 1). Structures for the 9:16 and 9:17 phases were proposed; both were based on a TTB-type host lattice of three subcells [as in Fig. 1(*c*)], and the different compositions were achieved by the partial filling of either eight (in 9:16) or ten (in 9:17) of the twelve possible pentagonal tunnels.

We anticipated that electron-optical observations of this material might yield useful additional information. In particular, high-resolution lattice images from thin fragments aligned with their *c* axis parallel to the electron beam should reveal the pattern of filled pentagonal tunnels. Also, the proposed long *c* axis of the domain unit cell, which was not observed in the X-ray data, should be more readily detected by electron diffraction.

We have now examined many fragments of $13Nb_2O_5.24WO_3$ obtained from Roth & Wadsley's (1965) collection, but have been unable to obtain confirmation of Stephenson's (1968) proposals. Apart from revealing a number of additional types of fault boundary, the lattice images appeared to be identical to those from $4Nb_2O_5.9WO_3$. Electron diffraction patterns showing the 00*l* reflexions contained no evidence for a superlattice or streaking which could be interpreted in terms of regular or semi-random stacking of slabs in the **c** direction. High-resolution electron microscopy of the specimens reported by Roth & Waring (1966) and used by Stephenson (1968) should throw additional light on this problem.

4. Discussion

4.1. *The technique*

We have endeavoured to derive structural models for several ordered and numerous more or less disordered TTB-type materials, by making direct correlations between contrast in high-resolution lattice images and elements of structure; in particular, occupied and empty tunnels. The validity of the procedure was checked by applying it first to the known structure of $4Nb_2O_5.9WO_3$, and it was extended to related structures only after ensuring that the experimental conditions (orientation, focus, crystal thickness) were reproduced as closely as possible. In most cases, the resulting structural models are convincing and, we believe, reliable, but this cannot be said for the reported phase '$6Nb_2O_5.11WO_3$', where the results appear to be at variance with previous X-ray work.

Although it is desirable in principle to compute the contrast expected from a postulated structural model for comparison with experiment, the calculations (O'Keefe, 1973) are relatively complex and time-consuming, and hardly seem necessary when one can compare contrast and structure for an analogous material of known structure. This approach seems to us to be particularly straightforward compared with any attempt to interpret an image in the absence of data on a closely related material of known structure. In the latter case, a calculation would be imperative, and it could be quite difficult to derive a plausible trial structure.

We are of the opinion that there are many cases which could be treated by an approach similar to the one we have described in this paper. The study of planar or linear faults in a matrix of known structure, and of order–disorder in the occupancy of sites or tunnels in an ordered host lattice, are obvious examples. However, it should be emphasized that disorder in the direction parallel to the incident electron beam will be difficult to resolve. In the present work, there is no evidence for disorder in the host lattice in this direction (*i.e.* parallel to **c**), but we are not confident that partially filled tunnels could be distinguished from fully occupied or empty ones. Cowley & Iijima (1972) have suggested non-linearity between image contrast and the projected potential of the crystal. Further calculations will probably be required in order to determine the relationship between contrast and the extent of occupancy of partially filled tunnels.

4.2. *The structures*

Our observations confirm that over the composition

range from about 64–78 mole % WO_3, the mixed oxides of hexavalent tungsten and pentavalent niobium exhibit structures which are based on a tetragonal tungsten bronze type of subcell, and that differences in composition are accommodated by varying the number of occupied pentagonal tunnels. The most important new piece of information is that the TTB-type host lattice appears to lose its stability when less than about one third of the pentagonal tunnels are occupied, and the structure is modified to include small regions of ReO_3-type material. This modification is periodic at the composition $2Nb_2O_5.7WO_3$, where one quarter of the TTB subcells are converted to ReO_3-type structure, and the proportion of occupied tunnels remains at one third [Fig. 6(*b*)] instead of being reduced to one quarter had the unmodified structure [Fig. 6(*a*)] been retained.

Thus the phase $2Nb_2O_5.7WO_3$ can be described as an ordered intergrowth of the TTB and ReO_3-type structures, and as such it may be regarded as a type of transition structure, lying between the pure TTB host lattice characteristic of several phases richer in Nb_2O_5, and the ReO_3 lattice (albeit interrupted by crystallographic shear planes) which appears at higher WO_3 contents (Roth & Waring, 1966; Allpress, 1972). As an intergrowth, if differs from those which occur so frequently in the block structures related to Nb_2O_5 (Andersson, Mumme & Wadsley, 1965; Allpress, 1969*b*). In the latter, the intergrowing components are slabs, which extend through the crystals in two dimensions, but have a restricted width. In $2Nb_2O_5.7WO_3$ on the other hand, the ReO_3-type regions are columnar microdomains, which extend in only one direction, along **c**, and are otherwise completely surrounded by the TTB-type matrix.

The occupancy of one third of the pentagonal tunnels may well be an optimum resulting from constraints on the filling of neighbouring tunnels. The geometry of the TTB lattice is such that each pentagonal tunnel has one neighbour at 0·61 nm distance, four at 0·65 nm, two at 0·92 nm, one at 1·15 nm, four at 1·22 nm, and four at 1·25 nm (these distances were derived from the data of Jamieson, Abrahams & Bernstein, 1968). In both the ordered structures [Figs. 1(*c*), 6(*b*)], nearest and second-nearest neighbour tunnels are never occupied simultaneously, and in addition, occupied tunnels may have one but never two occupied third-nearest neighbours (0·92 nm). If we construct a model which is as close packed as possible within these constraints, we obtain the 4:9 structure [Fig. 1(*c*)] directly. Within fault boundaries and in disordered materials (Fig. 10), the restriction on third-nearest neighbours is relaxed, and in the case of faults in the 4:9 phase, second-nearest neighbour tunnels are sometimes occupied simultaneously [*e.g.* Fig. 4(*b*)].

Roth & Waring (1966) described a metastable apparently disordered TTB-type phase '$3Nb_2O_5.8WO_3$', having no superlattice detectable by X-ray powder methods (Table 1). Its composition lies between those of $4Nb_2O_5.9WO_3$ and $2Nb_2O_5.7WO_3$, and after prolonged heating above about 1600°K it decomposes into these two ordered phases. We suspect that the lattice image in Fig. 10, which was recorded from a fragment whose nominal composition ($17Nb_2O_5.48WO_3$) lies close to that of this metastable phase, gives a good indication of the type of structure to be expected in this region. Previous work (Allpress, 1969*a*) has shown that 'single-crystal' electron diffraction patterns from fragments in this composition range exhibit sharp reflexions corresponding to the TTB-type subcell, surrounded by distinctive patterns of diffuse scattering. The latter were attributed to short-range order, and the present results provide direct confirmation that the structure consists of an ordered TTB-type host lattice, in which the occupancy of pentagonal tunnels is more or less random, and recognizable ordered regions of both $4Nb_2O_5.9WO_3$ and $2Nb_2O_5.7WO_3$ exist as minute domains of a few unit cells at most.

4.3. *The fault boundaries*

We have noted that constraints on the occupancy of pentagonal tunnels in fault boundaries are slightly less rigid than in the ordered structures. This implies that there is an energy associated with the boundaries, and that their elimination will be a thermodynamically favourable process. In the extreme case, the decomposition of the metastable '$3Nb_2O_5.8WO_3$', which we have referred to in the preceding section, is an example of this.

It is of interest to examine the reason for the presence of these boundaries, and it seems most likely that they are a consequence of the way in which the structures develop during the reaction of the component oxides. Let us assume that domains of ordered structure are formed by a nucleation and growth process, involving the simultaneous reorientation of octahedra in the ReO_3-type matrix of WO_3, and penetration of niobium and additional oxygen into the product lattice. The growing domains will eventually impinge upon one another, and unless they are in phase, a boundary of some kind will be formed between them. If the domains are out-of-phase by an integral number of subcell vectors, the boundaries will be simple out-of-phase boundaries (*e.g.* Figs. 3, 7) but if they are displaced by a half-integral number of subcell vectors [*e.g.* Figs. 4(*b*), 9] an additional mirror relationship between them is involved.

Apart from accommodating discrepancies of phase, fault boundaries may also act as sinks for the accumulation of non-stoichiometry. It appears that the boundary shown in Fig. 8 has this sole function, since the adjoining domains are exactly in phase with one another. Out-of-phase boundaries may also be associated with non-stoichiometry, and examples are shown in Figs. 3, 4 and 9(*b*).

Within the boundaries themselves, there is a remarkable degree of order, such that in general, unless a boundary changes direction, its structure tends to be strictly periodic. This observation indicates that there

is a strong tendency for what might be called microstructural order; *i.e.* once a configuration of domains is established during the reaction, the boundaries between them will tend to take up directions and structures in which the discrepancies of phase and/or composition are accommodated with the maximum possible degree of local order. The elimination of all these boundaries will inevitably require very much more extensive migration of the contents of occupied tunnels, either *via* interstitial sites, or involving exchange with sites in the host lattice. In the case of $2Nb_2O_5.7WO_3$, this migration will be accompanied by the reorientation of elements of the host lattice, in order to produce the required arrangement of 4×4 ReO_3-type blocks. In view of these extensive movements, and the relatively weak long-range forces between occupied tunnels, these processes are likely to be slow, and it is therefore not surprising that large numbers of fault boundaries have been observed, particularly in $2Nb_2O_5.7WO_3$. These conclusions could probably be verified by examination of a series of specimens heat-treated for varying periods of time and/or varying temperature to demonstrate the method of approach to equilibrium.

One of us (S.I.) wishes to thank Professor J. M. Cowley for his continuous encouragement, and to acknowledge the support of a N.S.F. Area Development Grant in Solid State Science (No. GU 3169).

References

ALLPRESS, J. G. (1969*a*). *Mater. Res. Bull.* **4**, 707–720.
ALLPRESS, J. G. (1969*b*). *J. Solid State Chem.* **1**, 66–81.
ALLPRESS, J. G. (1972). In Natl. Bur. Stand. Spec. Publ. 364, *Solid State Chemistry. Proceedings of the 5th Materials Research Symposium.* Edited by R. S. ROTH and S. J. SCHNEIDER.
ALLPRESS, J. G., SANDERS, J. V. & WADSLEY, A. D. (1969). *Acta Cryst.* B**25**, 1156–1164.
ANDERSSON, S., MUMME, W. G. & WADSLEY, A. D. (1965). *Acta Cryst.* **21**, 802–808.
COWLEY, J. M. & IIJIMA, S. (1972). *Z. Naturforsch.* **27***a*, 445–451.
CRAIG, D. C. & STEPHENSON, N. C. (1969). *Acta Cryst.* B**25**, 2071–2083.
IIJIMA, S. (1971). *J. Appl. Phys.* **42**, 5891–5893.
IIJIMA, S. (1973). *Acta Cryst.* A**29**, 18–24.
IIJIMA, S. & ALLPRESS, J. G. (1973). *J. Solid State Chem.* **7**, 94–105.
IIJIMA, S. & ALLPRESS, J. G. (1974). *Acta Cryst.* A**30**, 29–36.
JAMIESON, P. B., ABRAHAMS, S. C. & BERNSTEIN, J. L. (1968). *J. Chem. Phys.* **48**, 5048–5057.
MAGNÉLI, A. (1949). *Ark. Kem.* **1**, 213–222.
O'KEEFE, M. A. (1973). *Acta Cryst.* A**29**, 389–401.
ROTH, R. S. & WADSLEY, A. D. (1965). *Acta Cryst.* **19**, 26–32.
ROTH, R. S. & WARING, J. L. (1966). *J. Res. Natl. Bur. Stand.* **70A**, 281–303.
SLEIGHT, A. W. (1966). *Acta Chem. Scand.* **20**, 1102–1112.
STEPHENSON, N. C. (1968). *Acta Cryst.* B**24**, 637–653.

Acta Cryst. (1974). A**30**, 29

Structural Studies by Electron Microscopy: Coherent Intergrowth of the ReO_3 and Tetragonal Tungsten Bronze Structure Types in the System Nb_2O_5–WO_3

BY S. IIJIMA*
Department of Physics, Arizona State University, Tempe, Arizona 85281, *U.S.A.*

AND J. G. ALLPRESS
Division of Tribophysics, CSIRO, University of Melbourne, Parkville, Victoria, 3052, *Australia*

(*Received* 4 *June* 1973; *accepted* 22 *June* 1973)

High-resolution lattice images from WO_3-rich compositions in the system Nb_2O_5–WO_3 contain direct evidence for the coherent intergrowth of extensive domains of several orientations of the ReO_3-type structure with the more complex tetragonal tungsten bronze-type structure. A model for the transformation between the two structure types is proposed.

1. Introduction

In a preceding paper (Iijima & Allpress, 1974), we have described high-resolution electron-optical observations of several phases in the system Nb_2O_5–WO_3, and shown how the direct correlation of image contrast with structural features can be used to derive reliable models for the structure of $2Nb_2O_5.7WO_3$, and of fault boundaries and intergrowths in this material and in $4Nb_2O_5.9WO_3$. The structure of $2Nb_2O_5.7WO_3$ can be regarded as an ordered intergrowth of minute domains of the ReO_3 and tetragonal tungsten bronze (TTB) structural types.

Some previous observations at lower resolution (Allpress, 1972*a*) revealed the occurrence of more extensive

* On leave from the Research Institute for Scientific Measurements, Tohoku University, Sendai, Japan.